RESOURCE GEOLOGY, *vol. 52, no. 4, 359–369, 2002*

Hydrothermal Gold Mineralization at the Rodnikovoe Deposit in South Kamchatka, Russia

Ryohei TAKAHASHI, Hiroharu MATSUEDA* and Victor M. OKRUGIN**

Department of Earth and Planetary Sciences, Graduate School of Science, Hokkaido University, Kita-ku, N10 W8, Sapporo 060-0810, Japan [e-mail: ryohei@ep.sci.hokudai.ac.jp]

* *The Hokkaido University Museum, Hokkaido University, Kita-ku, N10 W8, Sapporo 060-0810, Japan*

** *Institute of Volcanology, FED Academy of Science Russian Federation, 9st Piip, 683006 Petropavlovsk-Kamchatsky, Russia*

Received on April 2, 2002; accepted on November 18, 2002

Abstract: The Rodnikovoe gold deposit situated in a presently active hydrothermal system located north of the Mutnovsko-Asachinskaya geothermal area in southern Kamchatka, Far Eastern Russia, consists of typical low-sulfidation quartz-adularia veins in a host rock of diorite. The age of the mineralization was dated by the K-Ar method as 0.9 to 1.1 Ma based on adularia collected from the veins. Representative ore minerals in the deposit are electrum, argentite, aguilarite, polybasite, pearceite and lenaite. Dominant alteration minerals are adularia, α-cristobalite, chlorite, illite and kaolinite. Hydrothermal solutions of neutral pH were responsible for the mineralization, which is divided into six stages defined by tectonic boundaries. Gold mineralization occurred in stages I and III. Hydrothermal brecciation occurred during stages III, IV and VI. Stages II, IV, V and VI were barren. The estimated ore formation temperature based on a fluid inclusion study is 150 to 250 ˚C at a depth of approximately 170 m below the paleo-water table. Boiling of hydrothermal fluids is hypothesized as the cause of the intermittent deposition of gold ore. The sulfur and oxygen fugacities during the deposition of anhydrite prior to the hydrothermal brecciation were higher than those during the gold mineralization stages. The occurrence in the hydrothermal breccia of fragments of high grade Au-Ag and polymetallic ores suggests that higher grade mineralization of these metal ores might have occurred in a deeper portion of the deposit.

Keywords: epithermal gold mineralization, boiling, hydrothermal brecciation, electrum, K-Ar age, fluid inclusion, physicochemical condition, Rodnikovoe, Kamchatka, Russia

1. Introduction

The Kamchatka Peninsula is rich in underground resources represented by gold, silver, platinum, zinc, lead, mercury, diamond, coal, gases and oil deposits. Estimated reserves in eight epithermal Au-Ag deposits of central and southern Kamchatka exceed 320 t Au and 2,000 t Ag (Liessman and Okrugin, 1994; Patoka et al., 1998; Stepanov et al., 2001). More than 15 t Au and 25 t PGE have been produced from placer deposits in the South Kamchatka area and the Vatynsko-Vyvensky sector of the Koryaksko-Kamchatsky Pt-rich belt at the northeastern part of Kamchatka (Okrugin, 1995).

The region is part of the arc-trench system of the Circum-Pacific belt. The subduction of the Pacific Plate beneath the Kamchatka Peninsula started in the Late Cretaceous, associated with an eastward migration of the magmatic arc. As a result, four NNE-trending volcanic chains have formed: Okhotsk-Chukotka (Late Cretaceous), Koryaksky-Western Kamchatka (Paleocene to Eocene), Central Kamchatka (Oligocene to Miocene) and Eastern Kamchatka (Pliocene to Recent). The present study area is situated in the Eastern Kamchatka Volcanic Belt (Fig. 1) where hydrothermal activity and related ore mineralization are abundant and well known in the Mutnovsko-Asachinskaya geothermal area (Vasilevsky et al., 1977a, b; Okrugin et al., 1994; Okrugin, 1995; Petrenko and Bolshakov, 1995; Petrenko, 1998, 1999).

The Rodnikovoe deposit located in the north of the geothermal area consists of typical low-sulfidation quartz-adularia-gold-silver veins. The largest vein is up to 25 m wide. Estimated reserves are 40.4 t Au (average grade 11.3 g/t) and 343 t Ag (average grade 95.8 g/t) (Patoka et al., 1998). A high grade Au-Ag ore sample (1,347 g/t Au, 10,000 g/t Ag) with visible gold was detected in a surface trench (Lattanzi et al., 1995; Petrenko, 1998, 1999; Stepanov et al., 2001).

In this paper, we document further characteristics of the Rodnikovoe deposit including mineralization stage, ore mineralogy, hydrothermal alteration and results of fluid inclusion thermometry. The physicochemical condition of the hydrothermal fluid, the mechanism of gold

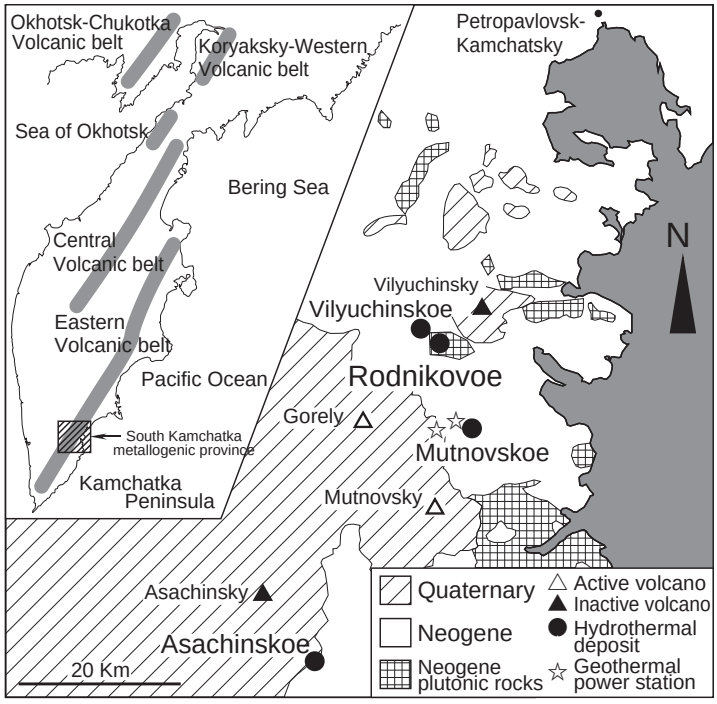

Fig. 1 Simplified geological map of the southern Kamchatka metallogenic province.

precipitation and the depth of mineralization relative to the paleo-water table are discussed.

2. Outline of Geology and Ore Deposits

2.1. Geology of the surrounding area

The Mutnovsko-Asachinskaya geothermal area is located 50-80 km south of Petropavlovsk-Kamchatsky (Fig. 1). The area is covered chiefly by Tertiary and Quaternary volcanic rocks. Petrenko (1998) reported that the volcanic rocks in South Kamchatka were formed in three stages of volcanism: Oligocene to Miocene (andesite), Late Miocene to Pliocene (basalt, andesite and rhyolite) and Quaternary (basalt and andesite). Sedimentary and volcanic rocks of Oligocene to Miocene are exposed along the east coast, and the ages of igneous rocks become younger towards the southwest. Subsurface igneous rocks related to the volcanism are plutons and dikes of gabbro, diorite, and andesite of Miocene to Pliocene age (Petrenko, 1998, 1999; Ministry of International Trade and Industry (abbreviated hereafter to MITI), 2001).

According to Kirsanov and Melekestsev (1991), volcanic activity of Mutnovsky Volcano (2,323 m) started in the Late Pleistocene with the latest phreatic eruption occurring in March, 2000 (Okrugin et al., 2001). According to a tephrochronological study (Melekestsev et al., 1987), volcanic activity of Gorely Volcano (1,829 m) started in the Early Pleistocene, resulting in the formation of four crater lakes. Ignimbrite emanating from Gorely Volcano now covers an area of approximately 600 km^2. The thickness of the deposit ranges from 5 to 30 m on the flank and from 300 to 350 m on the periphery (Melekestsev et al., 1987).

2.2. Ore deposits

In addition to the Rodnikovoe deposit, the Vilyuchinskoe, Mutnovskoe and Asachinskoe deposits are known in the Mutnovsko-Asachinskaya area (Fig. 1).

The Vilyuchinskoe deposit hosted by Pliocene volcaniclastic rocks consists of quartz veins that formed in faults mostly trending NE-SW and NNW-SSE (Petrenko and Bolshakov, 1995; Petrenko, 1998, 1999; MITI, 2001). The average grade of the Vilyuchinskoe ore is 10.3 g/t Au and 66 g/t Ag (Patoka et al., 1998). This deposit is located closely to the Rodnikovoe deposit, but the vein orientations and mineral assemblages differ.

The Mutnovskoe deposit is hosted by a series of Tertiary and Quaternary formations: Miocene to Pliocene sedimentary and igneous rocks, Pliocene dacite, rhyolite and rhyolitic tuff, and Pliocene to Pleistocene volcaniclastic rocks, gabbro and diorite. The gabbro and diorite are related to the mineralization. The deposit is composed of two parts: southern polymetallic Cu-Pb-Zn veins and northern Au-Ag quartz veins (Loshakov et al., 1974; Liessman and Okrugin, 1994; Lattanzi et al., 1995; Okrugin, 1995; Petrenko and Bolshakov, 1995; Petrenko, 1998, 1999; MITI, 2001).

The Asachinskoe deposit is hosted by Oligocene to Miocene andesite and Late Miocene to Pliocene basalt, andesite and rhyolite, all overlain by Pleistocene basalt and andesite. The mineralization is of quartz-adularia type associated with Au and Ag selenides. The estimated ore reserve is 1.30 Mt with 30.4 g/t Au and 58.5 g/t Ag (Petrenko, 1998; Sepeda et al., 1998).

3. Rodnikovoe Deposit

3.1. Outline of ore deposit

The Rodnikovoe quartz-adularia vein-type Au-Ag deposit is located in the vicinity of the Vilyuchinskie hot springs. The deposit is hosted by diorite, which possibly represents a subvolcanic magma chamber of Miocene to Pliocene age (Lattanzi et al., 1995). Middle Pleistocene ignimbrite effused from Gorely Volcano to form a 100 m thick layer overlying the diorite (Fig. 2). A small unit of Late Pleistocene to Holocene basaltic

andesite lava from Vilyuchinsky Volcano occupies the south of the area, shown in Figure 2 (Liessman and Okrugin, 1994; Okrugin et al., 1994; Okrugin, 1995).

Fig. 2 Geological map of the Rodnikovoe deposit (modified after Okrugin, 1995).

The ore body is exposed on the northern slope of the Vilyucha River valley at an altitude of 230 mL. There are three adits, designated Adit 1, Adit 2 and Adit Ort. Adit 1 is located 200 m east of Vein No. 44. Water vented from a hot spring precipitating carbonate scale is flowing out from Adit 1. A trench numbered 7 (designated here as Trench 7) into Vein No. 43 yielded several pieces of a range of high grade Au-Ag ores (Fig. 4-A). Strikes of the major veins are almost N-S, changing to NNW-SSE in the north of the area. Drilling exploration revealed that the major veins dip almost vertical (80-90° W), whereas smaller veins to the west of the major veins dip 45-80° E (Fig. 3).

3.2. Mineralization stages

Mineralization in Vein No. 44 is divided into six stages defined by tectonic boundaries. Furthermore, sub-stages are decided by growth boundaries in each stage. The mineral assemblage of each mineralization stage and sub-stage is

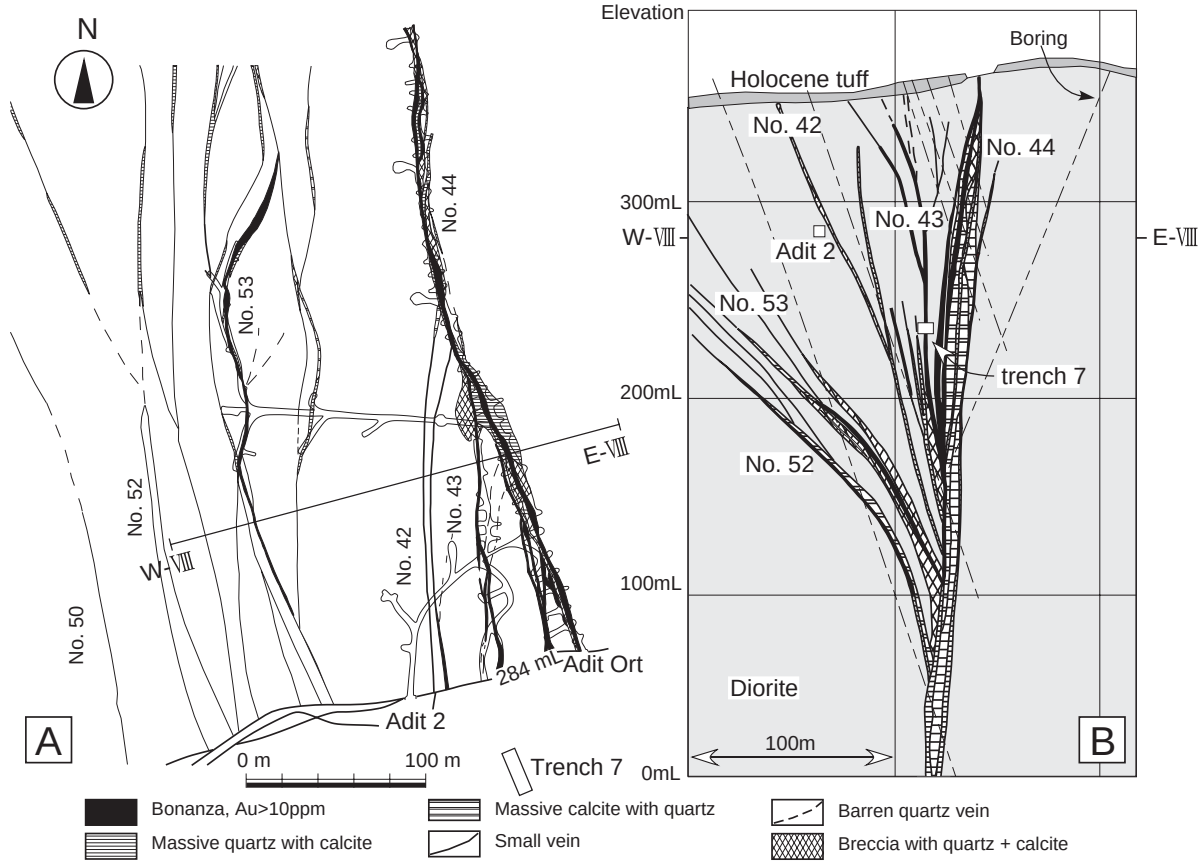

Fig. 3 Horizontal section (A) and cross section (B) of the Rodnikovoe deposit (after Okrugin, 1995). The virtual positions of Adit 2, Adit Ort and Trench 7 are projected on the sections.

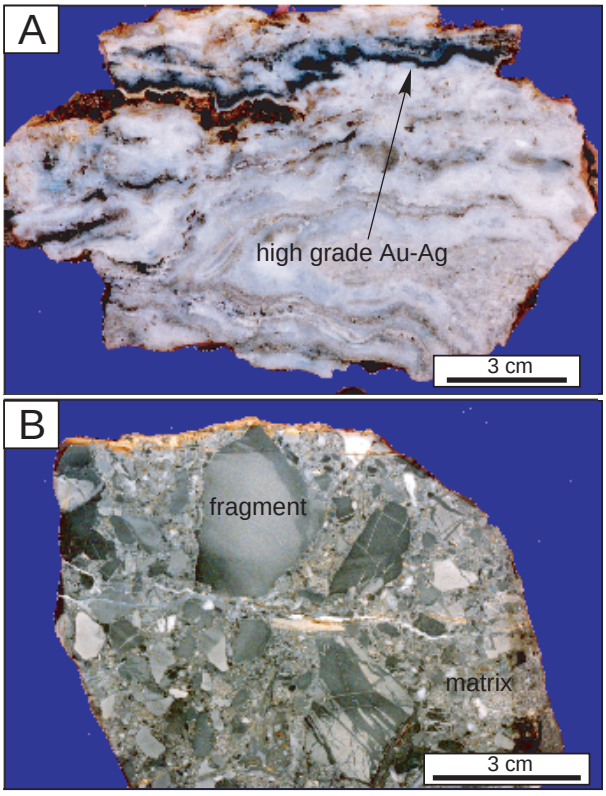

Fig. 4 Photographs of representative ores from the Rodnikovoe deposit. (A) High grade Au-Ag quartz of Vein No. 44 from Adit Ort. (B) Hydrothermal breccia from Vein No. 44. Each bar is 3 cm long.

shown in Figure 5.

Gold mineralizations occur intermittently in stages I and III. Formation of hydrothermal breccias occurs in stages III, IV and VI. Stage II consisting of pyrite and anhydrite is barren. Stages IV and V are represented by veinlets, cutting across ores of the earlier stages. Stage VI consists of calcite. Ores collected from an outcrop of Vein No. 44 near Adit Ort show high Au-Ag grades; based on field evidence and mineral assemblages, they were probably formed in stage III (designated here as stage III-n). Representative ore minerals in Vein No. 44 are electrum, argentite-aguilarite, polybasite-pearceite solid solution, lenaite, pyrite, chalcopyrite and sphalerite. Major gangue minerals are quartz, adularia, calcite and clay minerals. Adularia tends to have precipitated just before and after the deposition of Au- and Ag-bearing minerals. Silicified tuffaceous rocks are found as fragments in breccia of the stages III-f and III-k.

Vein No. 43 in Trench 7 is supposed to consist of stages III and VI. Stages III-α and III-β represent high grade Au-Ag mineralization associated with quartz and adularia, while stage III-γ is characterized by sphalerite, pyrite and quartz. Stages III-β and III-γ occur only as fragments in the breccia of stage VI-ε. Some ore fragments included in stage VI-ε at Trench 7 might have been derived from a deeper portion of the ore body.

K-Ar ages of adularia for stages I-a and III-k from Vein No. 44 are determined as 1.1±0.1 and 1.0±0.1 Ma, respectively (Table 1). The K-Ar age obtained for stage

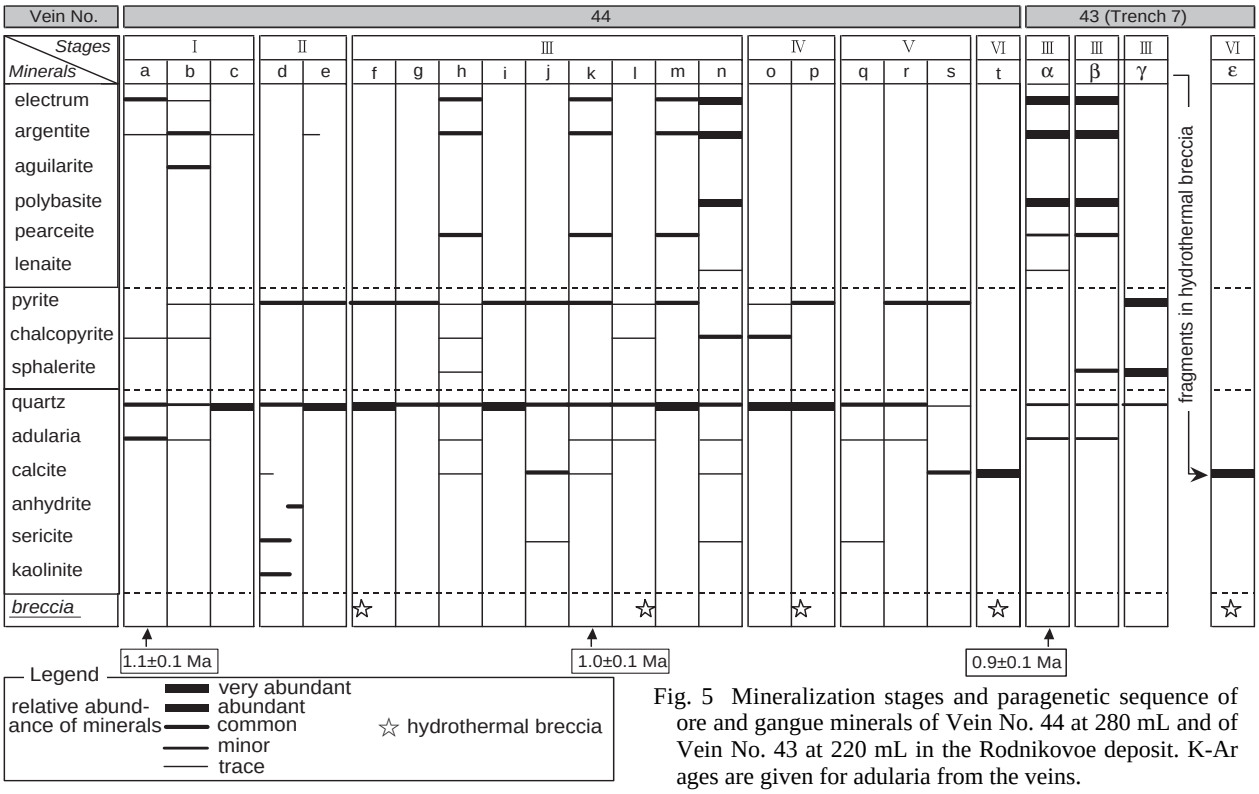

Fig. 5 Mineralization stages and paragenetic sequence of ore and gangue minerals of Vein No. 44 at 280 mL and of Vein No. 43 at 220 mL in the Rodnikovoe deposit. K-Ar ages are given for adularia from the veins.

Table 1 Results of K-Ar dating for adularia from the Rodnikovoe deposit.

No.	sample name	Age Ma	^{40}*Ar/^{40}K	^{40}*Ar ppm	^{40}*Ar/Total^{40}Ar	Ave.^{40}*Ar ppm	^{40}K %	Ave.^{40} K %	^{40}K ppm	Mineral
1	KR-1A	0.9±0.1	0.000053	0.000273	0.029	0.000292	4.607	4.605	5.494	adularia
				0.000311	0.026		4.603			
2	R1007-9	1.0±0.1	0.000061	0.000341	0.024	0.000358	4.892	4.919	5.868	adularia
				0.000374	0.011		4.946			
3	R1008-1	1.1±0.1	0.000065	0.000317	0.018	0.000278	3.546	3.608	4.305	adularia
				0.000271	0.018		3.671			
				0.000247	0.018					

III-α (0.9±0.1 Ma) is not consistent with the age of 2.7±1.0 Ma reported by Petrenko (1999). Field evidence and mineral assemblages indicate that stage III-α of Vein No. 43 corresponds to the later part of stage III as defined in Vein No. 44.

3.3. Mineralogy

3.3.1. Electrum: Grain sizes of electrum from Vein No. 43 differ from those of Vein No. 44, with ranges of 7-552 μm (av. 60 μm) and 5-39 μm (av. 14 μm), respectively. The chemical composition of electrum varies with respect to the mineralization stage. The Ag/(Au+Ag) atomic ratio of electrum decreases as mineralization proceeds during stage I (Fig. 6); by the beginning of stage III, it has a wide range of composition (45-59 atom% Ag). Thereafter, the electrum keeps a narrow range of composition (48-55 atom% Ag). On the other hand, electrum from stage III-n of Vein No. 43 and from stages III-α and III-β of Vein No. 43 show wide ranges of composition (Fig. 6).

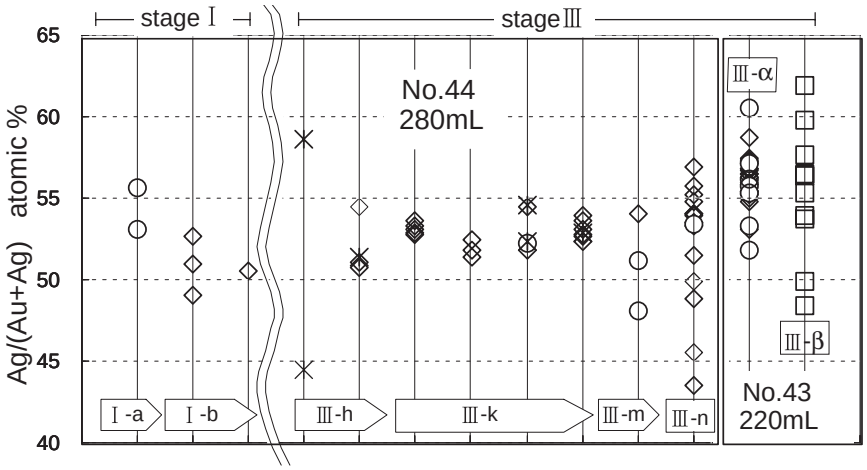

Fig. 6 Compositional variation of electrum with respect to mineralization stage. Each electrum coexists with argentite-aguilarite in each stage. The symbols indicate conterminous associations as follows: rhombuses (◇): electrum isolated, circles (○): electrum in contact with argentite-aguilarite, squares (□): electrum in contact with large amounts of argentite-aguilarite and polybasite-pearceite, crosses (×): electrum in contact with argentite-aguilarite, polybasite-pearceite, pyrite, chalcopyrite and sphalerite.

A sample of massive Ag-sulfide ore (2 × 2 × 2 cm) occurring as a fragment in the hydrothermal breccia in Vein No. 43 contains electrum expressed as coarse grains having a heterogeneous composition. Here, electrum fills the interstices between euhedral quartz crystals (Fig. 7).

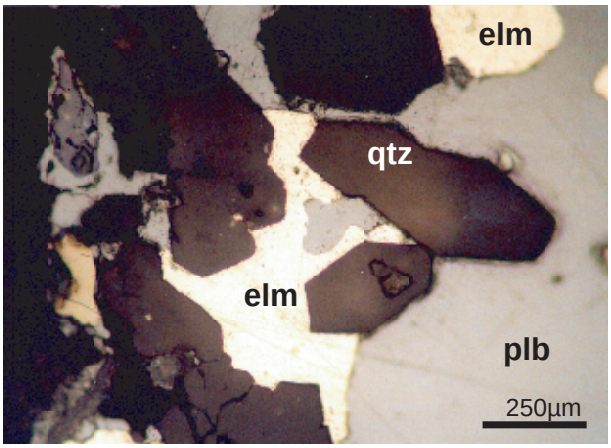

Fig. 7 Photomicrograph of electrum (elm) and polybasite (plb) filling interstices between euhedral quartz (qtz) crystals. This sample occurs as a fragment of hydrothermal brecciation of calcite from Trench 7 along Vein No. 43.

3.3.2. Ag minerals: Grain sizes and the Se/(S+Se) atomic ratios of argentite-aguilarite also differ between Veins No. 43 and No. 44. The ranges of grain size here are 16-110 μm (av. 53 μm) and 12-35 μm (av. 24 μm), respectively, with Se/(S+Se) atomic ratios of 0.06-0.1 (av. 0.08) and 0.14-0.39 (av. 0.23).

The Se/(S+Se) atomic ratios of polybasite-pearceite solid solution are 0.02-0.05 (av. 0.02) in Vein No. 43 and 0.05-0.07 (av. 0.06) in Vein No. 44.

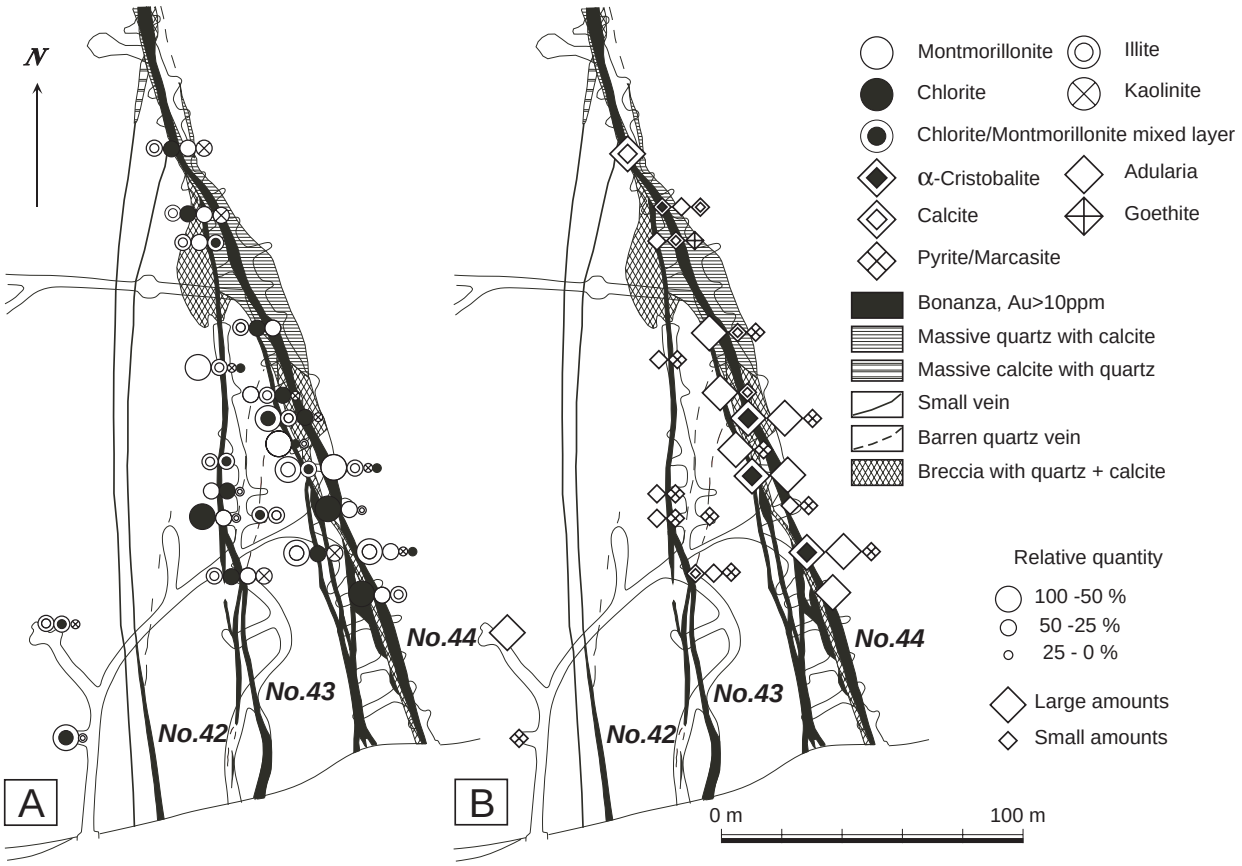

Fig. 8 Hydrothermal alteration map for the horizontal section at 280 mL of the Rodnikovoe deposit. Distribution of clayey minerals is shown in A, and other minerals in B.

Lenaite ($AgFeS_2$) occurs in stage III-n in Vein No. 44 and in stage III-α in Vein No. 43. Its grain size is 20 μm on average, with a maximum of 35 μm. Selenium was not detected in the lenaite. Under the microscope, lenaite exhibits a gray to white color with strong anisotropism; there is vivid internal reflection on a rough crystal surface (Amuzinsky et al., 1995).

3.3.3. Anhydrite: Anhydrite was detected by Laser Raman microspectrometry in stage II-d in Vein No. 44. It occurs as inclusions in comb quartz, and exhibits acicular or prismatic crystal form with on average 10-20 μm long crystals. The crystals seem to be primary inclusions distributed along growth planes of quartz crystals.

4. Hydrothermal Alteration

4.1. Analytical methods

In order to investigate hydrothermal alteration, samples were collected from argillic parts of wall rocks in contact with veins. The samples were separated into fractions of 1-5 μm in diameter. Representative specimens were treated with ethylene glycol for swelling, and with HCl for unconfirmed minerals having d-spacing at 7 Å. The specimens were measured with an X-ray diffractometer. The relative quantity of clay minerals (montmorillonite, illite, chlorite and kaolinite) was estimated based on the fundamental parameter method (Scafe and Kunze, 1971; Oinuma et al., 1972). Regular-type mixed-layer illite/ montmorillonite is rare, and the estimated content of montmorillonite is less than 5 %. Yet using visual inspection method (Higashi, 1980; Shirozu, 1988), the estimated content of chlorite in chlorite/montmorillonite mixed-layer mineral exceeded by 5 %.

4.2. Mineral association

The argillic parts consist of montmorillonite, chlorite, chlorite/montmorillonite mixed-layer mineral, illite, adularia, α-cristobalite, kaolinite, calcite, pyrite and marcasite (Fig. 8). Adularia is dominant in Vein No. 44, and α-cristobalite has not been detected in Vein No. 43. The alteration halo is wider around Vein No. 44 than that around Vein No. 43. Petrenko and Ozornin (1998) reported that the hydrothermal alteration zoning progressed horizontally from the periphery towards the vein zone as follows: 1) epidote-chlorite-actinolite, 2) fluorite-carbonate-epidote-illite, 3) illite-kaolinite and quartz-illite-adularia and 4) adularia-quartz.

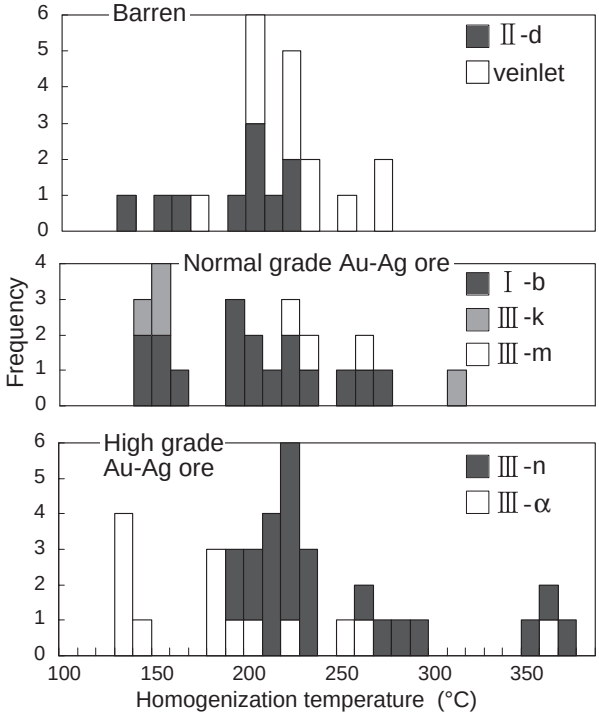

Fig. 9 Homogenization temperatures of fluid inclusions. The sample of veinlet was collected at 220 mL, 200 m east of Vein No. 44. The barren ore contains no Au-Ag minerals, and the normal grade Au-Ag ore contains Au-Ag minerals only seen by microscope observation. The high grade Au-Ag ore contains black tint bands of Au-Ag minerals on visual inspection and/or visible-sized Au-Ag minerals.

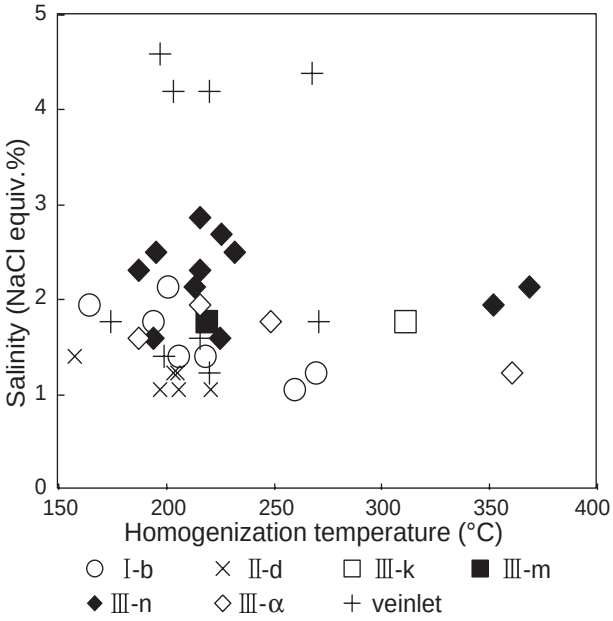

Fig. 10 Salinity vs. homogenization temperature of fluid inclusions.

5. Fluid Inclusions

5.1. Analytical methods

Microthermometry was carried out for primary fluid inclusions in quartz from the Au- and Ag-bearing veins and a veinlet recognized in Adit 1, located 200 m east of Vein No. 44 at 240 mL. The rising temperature rates were 0.1-0.3°C/min for ice melting and 1-3°C/min for homogenization.

Laser Raman analysis carried out at Fukuoka University was unable to detect gas components in fluid inclusions in the quartz, except for H_2O.

5.2. Microthermometry

As shown in Figure 9, fluid inclusions in the higher grade ores tend to show higher maximum homogenization temperatures. Vapor-rich inclusions observed in quartz of stages I-b, III-k, III-n and III-α suggest boiling phenomena. The boiling temperatures were estimated to be approximately 150°C for stages I-b, III-k and III-α and 200°C for stage III-n. The ranges of mineralization temperatures were estimated to be 180-230°C for stage II-d and 220-260°C for stage III-m.

Salinities of the fluid inclusions from the Au- and Ag-carrying veins were 1-3 wt% NaCl equivalent, whereas those from the veinlet were divided into two populations. The homogenization temperature and salinity data for stage I-b showed a slightly negative trend (Fig. 10).

6. Discussion

6.1. Physicochemical conditions

Figure 11 demonstrates the log f_{S_2} and temperature conditions estimated by the fluid inclusion data, the electrum-tarnish method (Barton and Toulmin, 1964), sphalerite geothermometer (Barton and Toulmin, 1966) and univariant mineral boundaries. As shown in this diagram, log f_{S_2} during gold mineralization stages was estimated to be -17 to -11 (atm).

Mineral boundaries and total concentrations of sulfur (logΣS) are shown on the log f_{S_2}- log f_{O_2} diagram at 200° C (Fig. 12-A). The estimated pH conditions are shown in the log f_{O_2}-pH diagram (Fig. 12-B). The logΣS at stage III-n was assumed to be approximately -2.5 to -1.5 (mol/kgH_2O) with log f_{S_2} equal to -13.5 to -11.5, resulting in log f_{O_2} equal to -44.5 to -42.5. The logΣS at stage II-d was assumed to be the same as at stage III-n. Boundaries of calcite-anhydrite were estimated by a reaction of $CaSO_4+CO_2 \leftrightarrow CaCO_3+1/2S_2+3/2O_2$ with fugacity variations of log f_{CO_2} ranging from -1.7 to 5.0 (Holland, 1965). The area of stage II-d shown on the diagram was estimated based on the logΣS range and

calcite-anhydrite boundary. The pH was lower and the sulfur and oxygen fugacities were higher in stage II-d (barren stage) than in stage III-n (gold precipitation stage) (Fig. 12). The higher oxygen fugacity might be caused by incorporation of oxidizing solution, suggested by the bimodal distribution of salinity data of fluid inclusions (Fig. 10).

Mineral boundaries, stability fields of the dominant sulfur species and solubility contours for gold complexes in ppb as $Au(HS)_2^-$ and $AuCl_2^-$ are shown in the log f_{O_2}- pH diagram at 200°C (Fig. 12-B). An ionic strength of 0.42 for stage III-n was applied in this assessment. The log f_{O_2} values were based on the log f_{S_2}-log f_{O_2} diagram (Fig. 12-A). The pH conditions for the assemblages of illite-adularia at stage III-n and of kaolinite-illite at stage II-d were estimated to be pH 6.16 and 4.52, respectively. The data shown in Figure 12-A indicate that the solubility of $Au(HS)_2^-$ was 100 to 1000 ppb in stage III-n. The solubility of $Au(HS)_2^-$ in stage II-d was approximately 10 to 100 ppb in the H_2S dominant condition, whereas it was quite low in the SO_4^{2-} - HSO_4^- dominant condition.

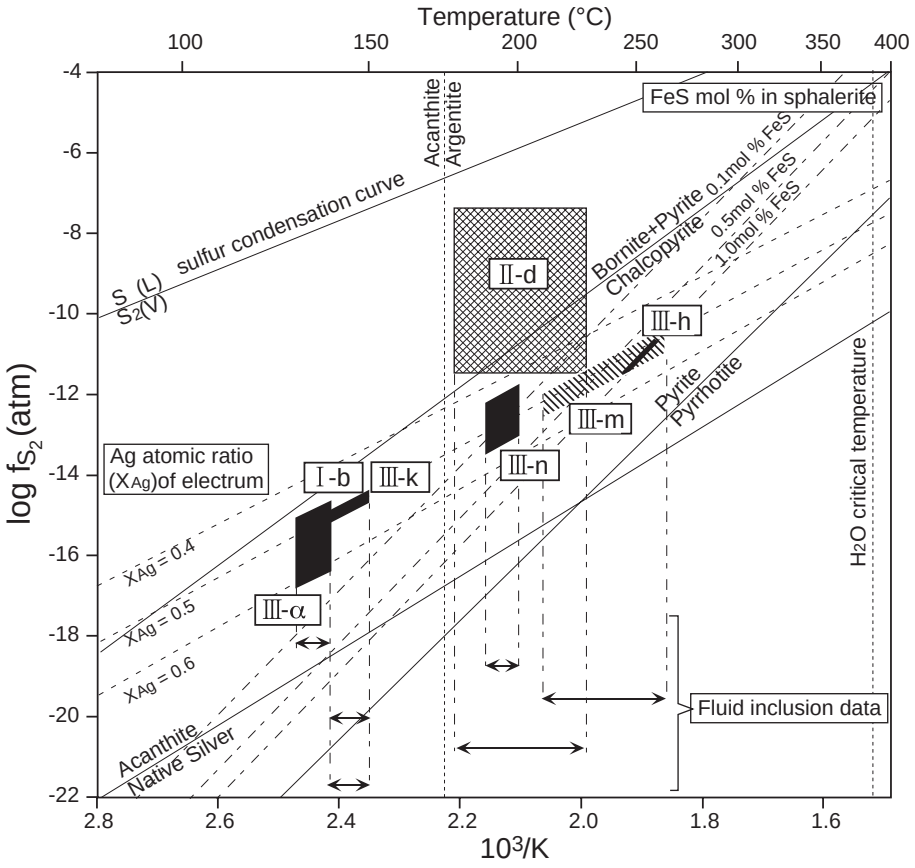

Fig. 11 Sulfur log f_{S_2} vs. temperature diagram of the mineralization stages. The estimations of each stage with the characteristics upon which they are based are as follows: stages I-b, III-k, stages III-n and III-α by the boiling temperatures of fluid inclusions and the electrum composition; stage III-m by the temperature range of fluid inclusions and the electrum composition; stage II-d by the temperature range of fluid inclusions and the estimated condition on the log f_{S_2} - log f_{O_2} diagram; and stage III-h by the composition of electrum and sphalerite. The univariant curves of argentite - native silver and sulfur condensation are quoted from Barton and Skinner (1967). The pyrite - pyrrhotite and bornite + pyrite - chalcopyrite curves are quoted from Scott and Barnes (1971).

6.2. Gold precipitation

Based on the fluid inclusion data and electrum-sphalerite geothermometry, the ore formation temperature was estimated to be from 150 to 250°C (Fig. 11). When the temperature is around 200°C and there are near neutral pH conditions, a supersaturation with respect to silica in the hydrothermal fluid is hypothesized (Izawa, 1985), which might be caused by boiling hydrothermal fluid. The mineral assemblage of stage III-n indicates that the fluid was weakly alkaline (Fig. 12-B). Under these conditions, gold is dissolved in the hydrothermal fluid to form the predominantly bisulfide thiocomplex $Au(HS)_2^-$ (e.g., Seward, 1973). Gold can be deposited from ascending hydrothermal fluid when boiling removes the CO_2 and H_2S from the water. The removal of CO_2 increases the pH of the hydrothermal solution and thus increases the solubility of $Au(HS)_2^-$. The removal of H_2S probably decreases the solubility of $Au(HS)_2^-$, leading to the precipitation of gold (e.g., Seward, 1989). The occurrence of gold (as electrum) has been identified from stages I-a, I-b, III-h, III-k, III-m, III-n, III-α and III-β (Fig. 5). Among these, evidence of boiling in fluid inclusions was observed in stages I-b, III-k, III-n and III-α. Thus, the deposition of gold was related to boiling of hydrothermal fluid.

Hydrothermal brecciation occurred during the hydrothermal activities deposited gold associated with boiling. Hydrothermal breccia is observed in stages III-f, III-k, IV-p and VI-t (Fig. 5). An event of hydrothermal brecciation is marked at the beginning of stage III (Fig. 5), subsequent to a tectonic boundary. This observation suggests that the hydrothermal brecciation event

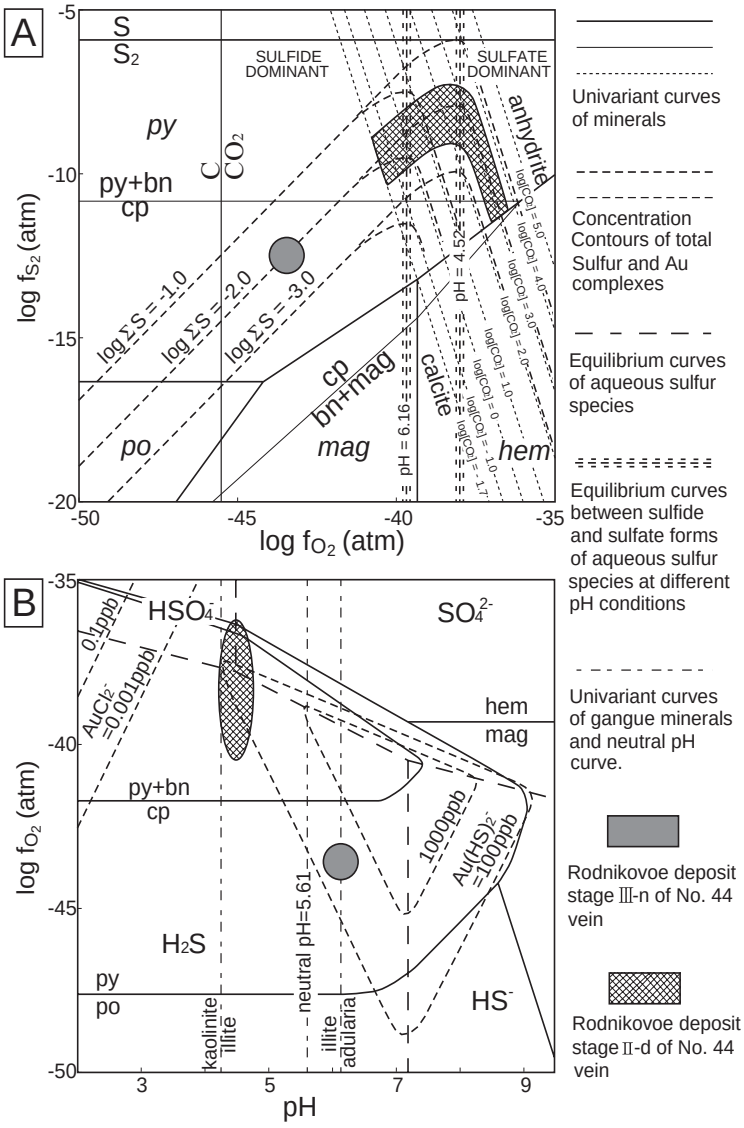

Fig. 12 (A) log f_{S_2} vs. log f_{O_2} and (B) log f_{O_2} vs. pH diagrams at 200°C, showing physicochemical conditions for the mineralization at stage III-n and stage II-d. Na-K-Ca geothermometers (Fournier, 1981) with a mean salinity of 2.5 and 1.2 wt% (NaCl equiv.) at stages III-n and II-d suggest calculated activities as follows: log[Na^+] = -0.67 and -0.93, log[K^+] = -2.03 and -2.28, log[Ca_2^+] = -5.13 and -5.63 and log[Cl^-] = -0.66 and -0.92, respectively. The total concentration of sulfur is expressed as logSS in mol/kgH_2O. The logΣS contours and the borders of the dominant aqueous sulfur species are shown with respect to pH conditions. The C-CO_2 boundary is put on the diagram (A) assuming f_{CO_2} where wollastonite is in equilibrium with calcite. The slide scale boundaries of calcite and anhydrite are from Holland (1965). The magnetite (mag) - hematite (hem), magnetite - pyrrhotite (po), chalcopyrite (cp) - pyrite + bornite and chalcopyrite (cp) - bornite (bn) + magnetite boundaries are from Helgeson (1969). The $Au(HS)_2^-$ contour is from Shenberger and Barnes (1989). The $AuCl_2^-$ contour is from Murray and Cubiciotti (1983). The kaolinite - sericite and sericite - adularia boundaries are from Arnorsson et al. (1982, 1983). Other data sets are quoted from Barton (1984).

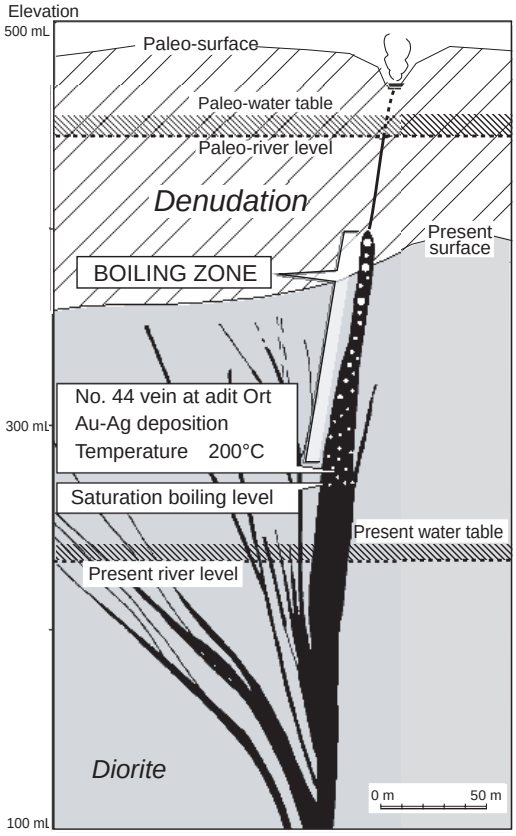

Fig. 13 A schematic model of gold deposition at Vein No. 44 in the Rodnikovoe deposit.

is also related to a choke of fractures. The choke of the hydrothermal fluid paths in the upper part of the ore body might have increased the pressure (Roedder and Bodnar, 1980), which, associated with an upward migration of the saturation boiling level, might have led to an event of hydrothermal brecciation.

6.3. Depth of mineralization

Veins are exposed inside Vilyucha River valley (Fig. 2); based on topography, denudation rates are assumed to be 0.1 mm/year at the ridges and 0.2 mm/year along rivers (Kaizuka, 1969). A schematic model of the hydrothermal system is constructed in Figure 13. High grade Au-Ag ore at stage III-n on 280 mL might have been formed at saturation boiling level. The formation temperature of 200°C at stage III-n at this altitude thus indicated a pressure of 15.6 bar. This gives a depth of 170 m below the water table under hydrostatic conditions (Haas, 1971). The depths during stages I-b and III-k on 280 mL indicating 150°C (Fig. 11) might therefore be above the saturation boiling level.

There are several differences between Veins No. 44 and No. 43: mineralization ages (1.1 to 1.0±0.1 and 0.9±0.1 Ma, respectively); the boiling temperatures (200 and 150°C, respectively); the higher Se/(S+Se) ratio in argentite-aguilarite and polybasite-pearceite solid solution in Vein No. 44; and the larger sizes of electrum and Ag-sulfides in Vein No. 43. Based on the boiling temperature at Vein No. 43 on 240 mL, the boiling pressure and corresponding hydrostatic depth were calculated to be approximately 4.8 bar and 40 m below the paleo-water table. Assuming that Vein No. 43 was formed after Vein No. 44, the level of the paleo-water table at stage III-α in Vein No. 43 on 240 mL might be approximately 160 m lower than that of stage III-n in Vein No. 44 on 280 mL.

7. Summary and Conclusions

K-Ar ages of adularia indicate 1.1 to 0.9±0.1 Ma for the gold mineralization stages at the Rodnikovoe deposit. The temperature range and pH of gold mineralization were estimated to be 150 to 250°C and neutral, respectively, indicating that $Au(HS)_2^-$ is the dominant dissolved form of Au. The gold ore body formed approximately 170 m below the paleo-water table. Intermittent precipitation of gold might be attributed to boiling of the ore fluid. Hydrothermal brecciation that occurred during the hydrothermal activity deposited gold associated with boiling. The occurrence of fragments of high grade Au-Ag and polymetallic ores in the hydrothermal breccia suggests that higher grade Au-Ag and/or polymetallic mineralization has formed at a deeper portion of this deposit.

Acknowledgments: The authors would like to express their sincere gratitude to Sachihiro Taguchi of Fukuoka University for the analysis of Laser Raman Spectrometry. We thank Shuji Ono of Hokkaido University for his cooperative field research in Kamchatka and fruitful discussions, and Srinivas Sarella for checking the English in this paper. We also extend our thanks to Takamura Tsuchiya, Anna Okrugina and Shunsuke Sakai for their helpful advice concerning this study, and Akira Imai and Eijun Ohta for their critical reviews.

References

Amuzinsky, V. A., Zhdanov, Y. Y., Zayakina, N. V. and Leskova, N. V. (1995) Lenaite $AgFeS_2$ - a new mineral species. Proc. Russian Mineral. Soc., 5, 85–91.

Arnorsson, S., Sigurdsson, S. and Svavarsson, H. (1982) The chemistry of geothermal waters in Iceland. I. Calculation of aqueous speciation from 0°C to 370°C. Geochim. Cosmochim. Acta, 46, 1513–1532.

Arnorsson, S., Gunnlaugsson, E. and Svavarsson, H. (1983) The chemistry of geothermal waters in Iceland. II. Mineral equilibria and independent variables controlling water compositions. Geochim. Cosmochim. Acta, 47, 547–566.

Barton, P. B., Jr. (1984) Redox reaction in hydrothermal fluid. *in* Henley, R. W., Truesdell, A. H. and Barton, P. B., Jr. (eds.) Fluid-Mineral Equilibria in Hydrothermal System. Rev. Econ. Geol., 1, 99–113.

Barton, P. B., Jr. and Skinner, B. J. (1967) Sulfide mineral stabilities. *in* Barnes, H. L. (ed.) Geochemistry of Hydrothermal Ore Deposits. 233–236, Holt, Rinehart and Winston, New York.

Barton, P. B., Jr. and Toulmin, P., III. (1964) The electrum-tarnish method for the determination of the fugacity of sulfur in laboratory sulfide system. Geochim. Cosmochim. Acta, 28, 619–640.

Barton, P. B., Jr. and Toulmin, P., III. (1966) Phase relations involving sphalerite in the Fe-Zn-S system. Econ. Geol., 61, 815–849.

Fournier, R. O. (1981) Application of water geochemistry to geothermal exploration and reservoir engineering. *in* Ryback, L. and Muffer, L. J. P. (eds.) Geothermal Systems. Chapt. 4, Principles and Case Histories, 109–143, Wiley, New York.

Haas, J. L. (1971) Effect of salinity on maximum thermal gradient of a hydrothermal system at hydrostatic pressure. Econ. Geol., 66, 940–946.

Helgeson, H. C. (1969) Thermodynamics of hydrothermal systems at elevated temperatures and pressures. Amer. Jour. Sci., 267, 729–804.

Higashi, S. (1980) Mineralogical studies of hydrothermal dioctahedral mica minerals. Mem. Fac. Sci. Kochi Univ., Ser. E, 1, 1–39.

Holland, H. D. (1965) Some applications of thermochemical data to problems of ore deposits II: Mineral assemblages and the composition of ore-forming fluids. Econ. Geol., 60, 1101–1166.

Izawa, E. (1985) Alteration zone and clay minerals in hydrothermal gold-silver deposits. - A speculation by the model of geothermal system. *in* Gold-Silver Ore of Japan. 3, 133–154, The Mining and Materials Processing Institute of Japan (in Japanese).

Kaizuka, S. (1969) Changing landforms - Under tectonic movement, sea level change and climatic change. Kagaku (Science), 39, 11–19 (in Japanese).

Kirsanov, I. T. and Melekestsev, I. V. (1991) Gorely Volcano. *in* Fedotov S. A. and Masurenkov, Y. P. (eds.) Active Volcanoes of Kamchatka. Vol. 2, Chapt. 27, 314–315, Moscow, Nauka Publ.

Lattanzi, P., Okrugin, V. M., Corsini, A., Okrugina, A., Tchubarov, V. and Livi, S. (1995) Base and precious metal mineralization in the Mutnovsky area, Kamchatka, Russia. Soc. Econ. Geol. News Letter, No. 20, 5-9.

Liessman, W. and Okrugin, V. M. (1994) Zur Lagerstaettenkunde der Halbinsel Kamchatka/Russland. Erzmetall, 47, 376–393.

Lonshakov, E. A., Vakin, E. A., Bocharova, G. I. and Okrugin, V. M. (1974) Volcanogenic ore vein of the Southern East Kamchatka. Geology. Geol. Rudnykh Mestorozheniy, 6, 121–125.

Melekestsev, I. V., Braitseva, O. A. and Ponomareva, V. V.

(1987) Dynamics of Mutnovsky and Gorely volcanoes activity during the Holocene and volcanic hazard in adjacent areas (based on the data of tephrochronology). Volcanol. Seismol., N3, 3–18 (in Russian).

Ministry of International Trade and Industry (2001) Far East Area. Researching Report of Satellite Image Analysis on 2000. Metal Mining Agency of Japan, 45p.

Murray, R. C., Jr. and Cubiciotti, D. (1983) Thermodynamics of aqueous sulfur species to 300°C and potential-pH diagrams. Jour. Electrochem. Soc., 130, 866–869.

Oinuma, K., Aoki, S. and Sudo, T. (1972) Problems of clay mineralogical study of marine sediments. Jour. Marine Geol., 8, 21–28.

Okrugin, V. M. (1995) Part 1. Mutnovsky Geothermal Field: Mutnovsky Hydrothermal Field Uzon-Geyser Depression. Post-Session Field Trip to Kamchatka. 8th Intern. Symp. Water-rock Interact., Vladivostok, Russia, 29p.

Okrugin, V. M., Kokarev, S. G., Okrugina, A. M., Chubarov, V. N. and Shuvalov, R. A. (1994) An unusual example of the interaction of a modern hydrothermal system with Au-Ag veins (South Kamchatka). Abstr. Goldschmidt Conference Edinburgh, Miner. Mag., 58A, 669.

Okrugin, V. M., Zelenskii, M. E., Marynova, V. K., Okrugina, A. M., Senyukov, S. L. and Sergeeva, S. V. (2001) Last news about volcanic activity in Kamchatka Peninsula: Mutnovsky and Gorely volcanoes especially. Proceedings of the Second International Workshop on Global Change: Connection to the Arctic, 2001. Bull. Research Center for North Eurasia and North Pacific Regions, Hokkaido University, 1, 146–163

Patoka, M. G., Litovinov, A. F. and Petrenko, I. D. (1998) Kamchatka - A new gold bearing province of Russia. Proceedings on Russian-Japanese Field Seminar -Mineralization Arc Volcanic-hydrothermal Systems (Kamchatka, Kuril and Japanese Isles). 72–75, Russia, Petropavlovsk-Kamchatsky.

Petrenko, I. D. (1998) Structural position of the gold - silver deposit of Southern Kamchatka ore field. *in* Present Hydrothermal Systems and Epithermal Gold-silver Deposits of Kamchatka (Field Excursion Guide), Chapt. 8, 65–67, Institute of Volcanology, Far East Division, Russian Academy of Sciences.

Petrenko, I. D. (1999) Gold-Silver Formation of Kamchatka. VSEGEI, S-Peterburg, 115p.

Petrenko, I. D. and Bolshakov, N. M. (1995) Structural position and age of Au-Ag mineralization of southern Kamchatka (Mutnovskoe ore field). Geol. Pacific Ocean, 5, 100–111.

Petrenko, I. D. and Ozornin, P. A. (1998) Rodnikovoe deposit. *in* Present Hydrothermal Systems and Epithermal Gold-silver Deposits of Kamchatka (Field Excursion Guide), Chapt. 9, 67–72, Institute of Volcanology, Far East Division, Russian Academy of Sciences.

Roedder, E. and Bodnar, R. J. (1980) Geologic pressure determinations from fluid inclusion studies. Ann. Rev. Earth Planet. Sci., 8, 263–301.

Scafe, D. W. and Kunze, G. W. (1971) A clay mineral investigation of six cores from the Gulf of Mexico. Marine Geol., 10, 69–85.

Scott, S. D. and Barnes, H. L. (1971) Sphalerite geothermometry and geobarometry. Econ. Geol., 66, 653–669.

Sepeda, A., Bolshakov, N. M. and Ozornin, P. A. (1998) Asachinskoe deposit and probable ways of development. *in* Present Hydrothermal Systems and Epithermal Gold-silver Deposits of Kamchatka (Field Excursion Guide), Chapt. 11, 78–82, Institute of Volcanology, Far East Division, Russian Academy of Sciences.

Seward, T. M. (1973) Thio complex of gold and the transfer of gold in hydrothermal ore solutions. Geochim. Cosmochim. Acta, 53, 379–399.

Seward, T. M. (1989) The hydrothermal chemistry of gold and its implications for ore formation: Boiling and conductive cooling as examples. Econ. Geol. Monogr., 6, 398–404.

Shenberger, S. D. and Barnes, H. L. (1989) Solubility of gold in aqueous sulfide solutions from 150–350°C. Geochim. Cosmochim. Acta, 53, 269–278.

Shirozu, H. (1988) Clay Mineralogy. Asaka Publ., 185p. (in Japanese).

Stepanov, I. I., Okrugin, V. M., Shuvalov, R. A. and Ananchenko, A. D. (2001) The relationship between mercury aureoles and occurrence on the territory of Kamchatka. Geol. Pacific Ocean, 16, 1161–1174.

Vasilevsky, M. M., Stefanov, Y. M., Shiroky, B. I., Kutyev, F. S. and Okrugin, V. M. (1977a) Metallogeny of Kamchatka upper structural story and the problem of ore specialization of folded regions tectonic-magmatic evolution. *in* Vasilevsky, M. M. (ed.) Forecasting Estimation of Ore Content of Volcanogenic Formation. 14–60, Nedra, Moscow.

Vasilevsky, M. M., Zimin, V. M. and Okrugin, V. M. (1977b) Volcanogenic ore centers of the southeastern Kamchatka. *in* Vasilevsky, M. M. (ed.) Inferred Reserves of Ore-bearing Volcanic Formation. 122–128, Nedra, Moscow.